A Study of Inkjet Printed Line Morphology Using Volatile Ink with Non-zero Receding Contact Angle for Conductive Trace Fabrication

Chenchao Shou, Patrick McCarthy, George T. C. Chiu, Timothy S. Fisher; Purdue University; West Lafayette, IN/USA

Abstract

Inkjet printed lines on a homogeneous solid substrate are studied under the condition that ink evaporation is not negligible and the contact angle exhibits hysteresis with non-zero receding contact angle (NRCA). A new family of line instability is discovered, featured by formation of agglomerations within a line. The agglomeration is explained by a flow that consistently drives a bead on the substrate towards fresh deposited drops due to concentration-induced surface tension gradient. Morphologies of lines printed with multiple layers are also investigated for the purpose of conductive trace fabrication. A non-uniform morphology is observed across a multi-layer line when the line is printed unidirectionally at a low jetting frequency. This non-uniformity is explained by considering interaction between deposited drops and bulk layer. Optimized multiple-pass printing is developed to produce a uniform line morphology while offering excellent printing efficiency and electrical conductivity.

Introduction

In the recent decade inkjet printing has been shown to have great potential to be used to fabricate fine conductive traces for electronic devices. Compared to conventional electronic fabrication techniques, such as photolithography and screen printing, inkjet printing has several advantages, including dramatically reduced manufacturing cost, excellent flexibility and efficient use of materials [1–3]. To print a smooth, narrow and highly conductive line on a dry homogeneous solid surface, however, is not a trivial task, which requires fundamental understanding of how printing parameters, like dot spacing and jetting frequency, influence the morphology of a printed line.

Much work has been dedicated to elucidating the conditions that lead to different types of printed line morphologies. Early theoretical work by S. Davis [4] showed that a liquid bead on a solid surface was stable only if the contact line was arrested and the contact angle was smaller than $\frac{\pi}{2}$. Duineveld [5] studied the stability specifically for inkjet printed lines, where he discovered that a printed line always broke up into individual drops on a substrate with non-zero receding contact angle (NRCA) but could either be stable or have bulging instability with zero receding contact angle (ZRCA) depending on the relative transported flow rate through the ridge to the applied flow rate. It's worth noting that the experiments conducted by Duineveld used an aqueous solution, which had a relatively low vapor pressure and his proposed theoretical model assumed that ink evaporation was negligible during the course of printing. Stringer and Derby [6, 7] extended the Duineveld's work by showing that the width of a stable line was always bounded by two limits. Soltman [8] studied the effect of substrate temperature on the printed line morphology with emphasis on how to suppress coffee ring effect. All the experiments in the work of Stringer, Derby and Soltman were conducted under ZRCA conditions. Therefore previous line morphology studies mainly focus on the scenarios where ink evaporation is negligible or the receding contact angle is zero. The effect of ink evaporation on the line morphology, especially with NRCA condition, has not been well studied to our best of knowledge.

In this paper we present an experiment-based study of printed line morphologies using a volatile organometallic compound solution. We will study single-layer printed lines, where the impact of ink evaporation and contact line depinning will be elucidated. Unlike the previous line morphology studies [5–8], here we will extend our discussion to the morphologies of lines printed with multiple layers. We are particularly interested in how the uniformity of multi-layer lines changes with different printing methods. Finally an optimized printing routine will be developed to achieve uniform morphologies with excellent performances in both printing efficiency and electrical conductivity.

Experiments

The ink used in this study is palladium hexadecanethiolate dissolved in toluene synthesized in-house with molar concentration of 32mM [9]. The substrates are SiO2/Si wafers (Nova Electronic Materials, Inc.), pre-cleaned in a sonication bath (Branson 2510) with 5 min acetone followed by 5 min isopropanol and then blown dry by compressed air. The ink properties are measured [10] and summarized in Table 1.

Table 1: Fluid Properties of the Ink Used in This Study

Ink properties	Values
Density, ρ (kg/m^3)	853.99
Surface tension, σ (mN/m) @ 25°C	24.312
Viscosity, μ $(mPa \cdot s)$	0.602 - 0.603
Advancing contact angle on SiO2/Si, θ_a (○)	13.7±1.9
Receding contact angle on SiO2/Si, θ_r (○)	9.6±1.7
Equilibrium contact angle on SiO2/Si, θ_e (○)	13.3

The inkjet printing system includes a linear positioning stage (Anorad-WKY-C-150) with an encoder resolution of 0.5μm and Hewlett Packard Thermal Inkjet Picojet System (HP TIPS).

The volume of a single droplet is about 45 pL, corresponding to in-flight droplet diameter D_i = 44 μm. The drop diameter D_0 on the SiO2/Si substrate is about 125 μm. The velocity of the droplet V_i as it impacts onto the substrate is measured to be 5.03 m/s. All the experiments are conducted at the room temperature.

Results and Discussions

Single-layer Printed Line Morphologies

Single-layer printed line morphologies are studied by varying dot spacing from 20 μm to 100 μm and changing time between depositions of adjacent drops from 2 ms to 350 ms.

Fig.1 shows the line morphologies with different time between adjacent drops when dot spacing is kept fixed at 70 μm. All the lines shown in Fig.1 are printed from left to right with respect to the substrate.

Based on distinct characteristics, the morphologies of single-layer printed lines are classified into three categories as the time between adjacent drops increases: (i) one or several agglomerations in the middle of the line with short time between adjacent drops ($<\sim$50 ms), as shown in Fig.1(a) and Fig.1(b); (ii) one agglomeration at the end of the printed line with perceptible ring formations across the line when the time between adjacent drops is medium ($\sim$50 ms to $\sim$250 ms), as shown in Fig.1(c)-(f); (iii) no perceptible agglomeration with long time between adjacent drops ($>\sim$250 ms) in Fig.1(g). Our experiments have shown that this classification of printed line morphologies based on time between adjacent drops is appropriate not only for dot spacing = 70 μm but for other dot spacing as well.

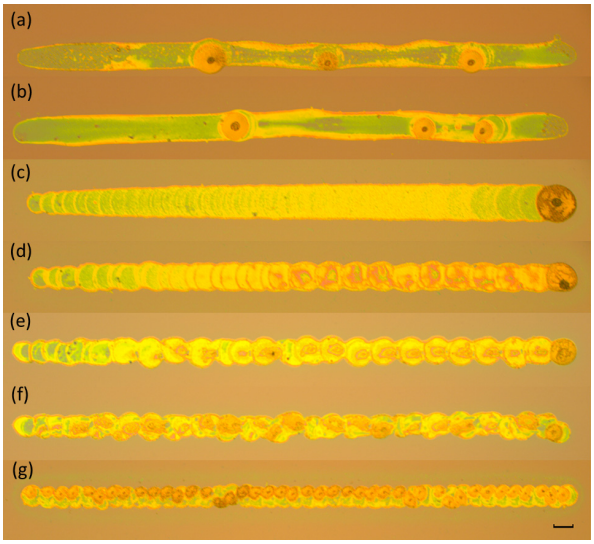

Figure 1. *Single-layer lines printed from left to right with dot spacing 70 μm, time between adjacent drops (a) 2 ms; (b) 10 ms; (c) 70 ms; (d) 100 ms; (e) 150 ms; (f) 200 ms; (g) 290 ms. The calibration bar represents 100 μm.*

It's worth pointing out that the location of the agglomeration within a line printed with medium time between adjacent drops only depends on the print direction. This is confirmed by the observation of an agglomeration at the left end of a line when the line is printed from right to left. Apparently ink tends to migrate to the end where the last drop is deposited when the time between adjacent drops is medium.

Explanation of Printed Line Morphologies with Medium Time between Adjacent Drops

When the second droplet impacts onto the first drop on the substrate, the first drop has already lost a considerable amount of volume due to the evaporation of the volatile solvent. To validate this argument, a simple and conservative estimation of the evaporation loss during the medium time between adjacent drops is performed. Simulation has shown that more than 99% of a drop is lost due to evaporation during the initial time period of 250 ms [10]. Even the smallest medium time between adjacent drops ($\sim$50 ms) is equivalently about 20% of this amount of time. Moreover, the evaporation rate of a drop on the surface decreases towards the end of evaporation process [11], which implies that the actual evaporation loss during the initial time period of 50 ms is greater than 20% of the volume of a single drop. Therefore the molar concentration (defined as the moles of the solute divided by the volume of the solution) of the first drop considerably increases when the second drop arrives.

Change in the molar concentration causes change in the surface tension. The relationship can be determined using Gibbs Adsorption Equation [12]:

$$d\gamma = -\sum_i \Gamma_i d\mu_i \tag{1}$$

where γ is the surface tension of a liquid, Γ_i and μ_i are respectively the surface excess and the chemical potential of the component i. The chemical potential of the component i is linearly dependent on the natural logarithm of its concentration.

The surface tension of the ink (24.312 mN/m) is measured to be smaller than that of pure toluene (27.73 mN/m [13]), of which the molar concentration is zero. This indicates that the surface excess of the solute must be positive. In other words, the surface tension of the ink decreases as the molar concentration increases.

Therefore when the second drop begins to merge with the first drop, the second drop has higher surface tension than the first drop. A flow induced by this surface tension gradient pulls the first drop towards the second drop. After the first two drops merge and equilibrate, the merged drop continues to evaporate before it makes contact with the third upcoming drop. Since the merged drop has higher molar concentration thus smaller surface tension than the third drop, the third drop pulls the merged drop to its side. The subsequently deposited drops follow this process and keep dragging the liquid bead on the substrate. Once the printing is finished, the bead evaporates completely, leaving a dense agglomeration at the end of the printed line. This explanation of concentration-induced surface tension gradient as a cause of a flow within a printed line was also used by Duineveld in his paper [5] to validate his model assumption of negligible ink evaporation during the course of printing.

Another essential fact that contributes to the ink migration is that the medium time between adjacent drops is actually long enough so that the liquid bead on the substrate has depinned from its contact line due to non-zero receding contact angle prior to merging with the next arriving droplet. One of the evidences that a bead has already depinned from its contact line is the circular ring formation along the contact line (i.e."coffee ring effect" [14]) and there are noticeable ring formations in the lines printed with medium time between adjacent drops (Fig.1(c)-(f)). A bead with a retreating contact line has low pinning forces on the solid surface thus facilitating the hydrodynamic pulling by a flow.

Based on the explanation above, the bead volume after every deposition can be modelled. To facilitate the formulation of the bead volume, some assumptions and simplifications are made:

- Time for a drop to reach its equilibrium state (i.e. form a spherical cap) is negligible, which is estimated to be less than 0.8 ms [15]. This amount of time is three orders of magnitude smaller than drop evaporation time ($>\sim$250 ms). Therefore evaporation during this period is negligible.
- Time for a bead on the substrate to merge with arriving droplet upon contact is negligible, which can be estimated by $0.5(\rho D_i^3/\sigma)^{0.5}$ = 27.4 μs [16]. Therefore evaporation during this period is negligible.
- Ink is an ideal solution. Hence liquid volumes are additive.
- Droplets arrive the substrate with constant volume.

Define the bead volume just after the n^{th} deposition V_n.

$$V_n = nV_0 - \sum_{i=1}^{n-1} \triangle V_{i,i+1}, V_1 = V_0 \quad (n = 2,3,4...) \tag{2}$$

where V_0 is the droplet volume prior to impact or merging, which has been assumed to be a constant. $\triangle V_{i,i+1}$ is the volumetric loss of the liquid bead due to evaporation from the i^{th} deposition to the $(i+1)^{th}$ deposition.

Rewrite Eq.2 in the form of the first order forward difference equation, we have

$$\triangle V_n = V_{n+1} - V_n = V_0 - \triangle V_{n,n+1} \quad (n \in \mathbb{N}^*) \tag{3}$$

$\triangle V_{n,n+1}$ by definition captures the amount of evaporation loss starting from a bead of a spherical cap with volume V_n for an extended period of time between adjacent drops τ thus is a function of V_n and τ.

$$\triangle V_n = V_0 - f(V_n, \tau) \quad (n \in \mathbb{N}^*) \tag{4}$$

Therefore the second order forward difference of the bead volume $\triangle^2 V_n$ can be expressed as

$$\triangle^2 V_n = \triangle V_{n+1} - \triangle V_n = f(V_n, \tau) - f(V_{n+1}, \tau) \quad (n \in \mathbb{N}^*) \tag{5}$$

Previous studies [11, 17] have shown that drop evaporation rate increases with drop base radius. The cube of the drop base radius is proportional to the bead volume. Hence the evaporation rate increases with the bead volume V_n. Within a printed line the time between adjacent drops τ is fixed. So the amount of evaporation loss $f(V_n, \tau)$ during the period of τ increases with V_n. Therefore when $\triangle V_n > 0$, we have $\triangle^2 V_n < 0$ (Eq.5). Physically this means that as the number of depositions increases, the bead volume after every deposition increases at a decreasing rate.

When the bead volume increases to such that the evaporation loss during the time between adjacent drops is equal to the arriving droplet volume, it reaches equilibrium. Mathematically it can be expressed as

$$V_0 = f(V_e, \tau) \tag{6}$$

where V_e is equilibrium bead volume.

If the bead volume overshoots the equilibrium (i.e. $V_n > V_e$), $f(V_n, \tau) > f(V_e, \tau)$. With Eq.4 and Eq.6, we have $\triangle V_n < 0$. Similarly if $V_n < V_e$, $\triangle V_n > 0$. This indicates V_e is a stable equilibrium.

Obviously the evaporation loss $f(V_n, \tau)$ increases with the time between adjacent drops τ when V_n is held constant. Therefore in order to maintain the equality of Eq.6, the equilibrium bead volume V_e must decrease as τ increases.

The bead leaves a circular ring at the edge after its contact line recedes. The diameter of the ring formed after the n^{th} deposition D_n can be related to the bead volume V_n by

$$V_n = \frac{\pi(1-\cos(\theta_e))^2(2+\cos(\theta_e))}{24(\sin(\theta_e))^3} D_n^3 = KD_n^3 \tag{7}$$

where θ_e is the equilibrium contact angle and K is a constant.

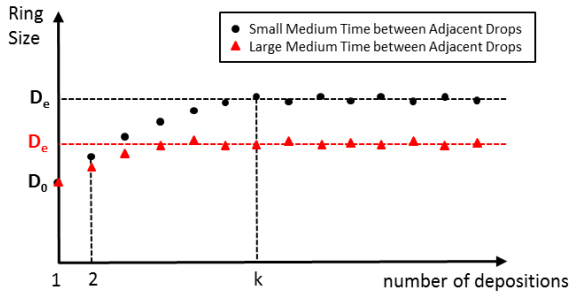

Figure 2. *Predicted changes of the ring sizes in a line with small or large medium time between adjacent drops. D_e is the equilibrium ring size and D_0 is the drop diameter.*

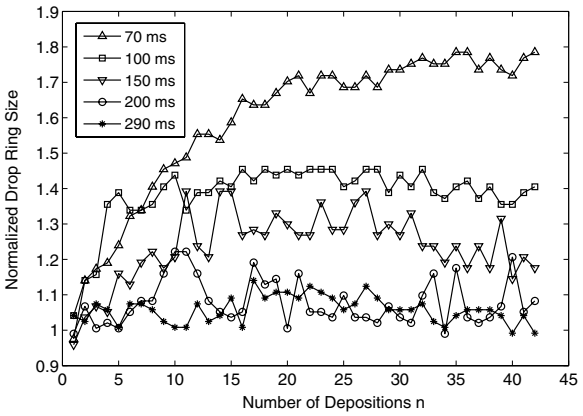

Figure 3. *Measured ring sizes in lines printed with different time between adjacent drops through analyzing optical images in Fig.1(c)-(g). The ring sizes are normalized with respect to the drop diameter.*

With cubic relationship between D_n and V_n as shown in Eq.7, it can be proved that the dynamics of the ring size D_n changing with the number of depositions follows the same trend as that of the bead volume V_n [15]. Therefore the change of the ring size with the number of depositions is predicted as in Fig.2, where D_e is the equilibrium ring size equal to $(V_e/K)^{1/3}$ and D_0 is the drop diameter equal to $(V_0/K)^{1/3}$.

The measured ring sizes across printed lines (Fig.3) reasonably agree with the predicted trend (Fig.2). The normalized ring sizes always start from about 1($< \pm 5\%$) for all the printed lines. This supports the prediction in Fig.2 that the ring size of the first deposition is always equal to the drop diameter.

Explanation of Printed Line Morphologies with Long Time between Adjacent Drops

When a line is printed with long time between adjacent drops, every drop has evaporated completely prior to the arrival of the next droplet. Therefore the volumetric loss due to evaporation during the time between adjacent drops is always equal to a single droplet volume (i.e. $\triangle V_{n,n+1} = V_0$). With Eq.3, we have $V_n = V_0$. Therefore the ring size across a printed line $D_n = (V_n/K)^{1/3} = D_0$ is a constant equal to the drop diameter. This reasonably agrees with the measured ring sizes in a line printed with 290 ms between adjacent drops (Fig.3).

Explanation of Printed Line Morphologies with Short Time between Adjacent Drops

When a line is printed with short time between adjacent drops, the first drop merges with the second drop while its contact line is still pinned (i.e. the contact angle is still larger than the receding contact angle). The evaporation loss during the time between adjacent drops is small because of the short time between adjacent drops. As a result, the surface tension gradient due to changes in molar concentration is weak. Therefore the ink migration with short time between adjacent drops is not as strong as that with medium time between adjacent drops.

The agglomerations in the middle of the line (Fig.1(a),(b)) are believed to result from complex competing dynamics between a flow due to surface tension gradient and time-varying pinning conditions of the contact line of the bead. However, the exact fluid dynamics that leads to the formation of those agglomerations is still unclear at present and requires further investigation.

Multi-layer Printed Line Morphologies

Multi-layer Line Morphologies with Short or Medium Time between Adjacent Drops

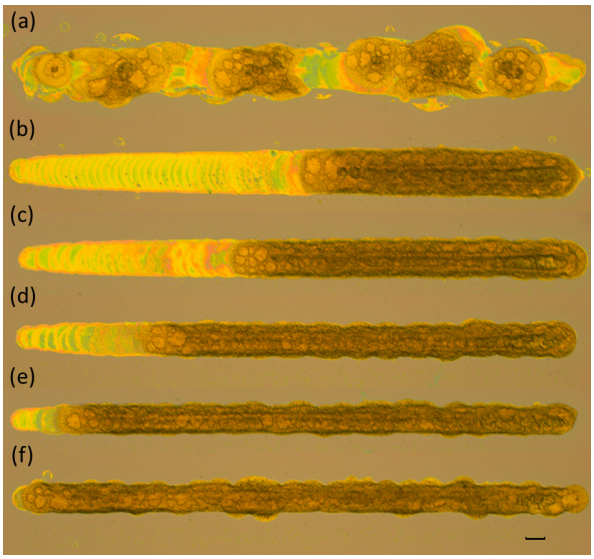

Figure 4. *15-layer lines printed unidirectionally from left to right with dot spacing 40 μm, time between adjacent drops (a) 10 ms; (b) 110 ms; (c) 130 ms; (d) 150 ms; (e) 170 ms; (f) 190 ms. The calibration bar represents 100 μm.*

When each layer is printed with short time between adjacent drops (Fig.4(a)), the line appears to be highly irregular with several perceptible agglomerations in the middle.

When each layer is printed with medium time between adjacent drops (Fig.4(b)-(f)), at the end of the line there is a dense agglomeration, the length of which grows with time between adjacent drops.

The agglomerations in those lines can be considered as the accumulation of agglomerations that take place at every layer.

Multi-layer Line Morphologies with Long Time between Adjacent Drops

The beginning of a multi-layer line appears to be darker than its end when the line is printed unidirectionally with long time between adjacent drops (Fig.5(a)). This non-uniformity becomes more profound as the number of layers increases.

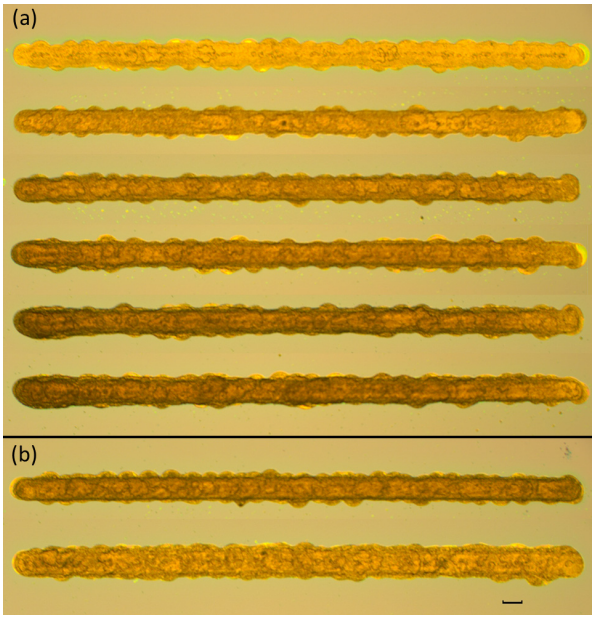

Figure 5. *(a) Multi-layer lines printed unidirectionally from left to right with dot spacing 40 μm, 290 ms between adjacent drops. The numbers of layers from the top line to the bottom line are 3, 5, 7, 10, 13 and 15. (b) Two 10-layer lines with dot spacing 40 μm. The first line is printed bidirectionally with 290 ms between adjacent drops. The second line is printed with 5 passes. The calibration bar represents 100 μm.*

The morphologies of those lines in Fig.5(a) can be explained by considering interaction between deposited drops and bulk layer. When a drop is deposited onto the bulk layer that has been previously laid down, unlike the case of printing a single-layer line where there is no mass exchange between drops and the substrate, it dissolves the bulk layer. After the drop completely evaporates, a crater-like hole is typically formed in the bulk layer [18, 19]. Since each layer is printed with long time between adjacent drops, a drop finishes evaporation process prior to the arrival of the next adjacent drop. When the next drop lands on the bulk layer, part of the drop falls and slips into the hole created by the previous drop due to gravity. The landed drop then dissolves the bulk layer underneath making the hole even wider and deeper. The whole process is illustrated in Fig.6(a).

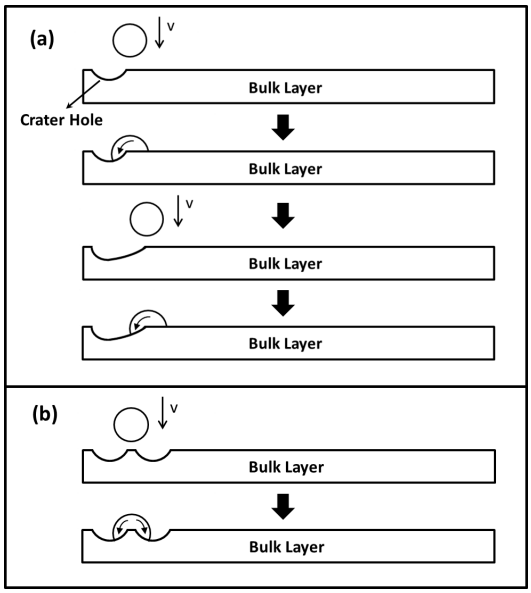

Figure 6. *A crater hole is formed in the bulk layer after a drop evaporates. (a) When a line is printed unidirectionally with long time between adjacent drops, deposited drops consistently slip into the hole due to gravity; (b) when a line is printed in multiple passes, the drops in one pass typically land on two holes created by the drops in the previous pass.*

After a full layer is deposited, the printed line has more material at the beginning than its end because of the ink migration through the slip motion of deposited drops into the hole. Furthermore, the beginning of the layer profile is the shallowest. This inclined profile facilitates the slip motion of the drops deposited in the subsequent layers with the same print direction. Therefore the extent to which the line exhibits non-uniformity grows as the number of unidirectionally printed layers increases (Fig.5(a)).

Multi-layer Line Morphologies with Bidirectional Printing or Multiple-pass Printing

The multi-layer lines printed bidirectionally or with multiple passes (Fig.5(b)) exhibit better uniformity than the unidirectionally printed line with the same number of layers (the fourth line from the top in Fig.5(a)).

When a line is printed bidirectionally with long time between adjacent drops, ink migration that results from deposition of odd layers is counterbalanced by that resulting from deposition of even layers. In this way the line uniformity is improved.

When the second line in Fig.5(b) is printed with multiple passes, which is also known as multilevel matrix [20], the time between any two consecutive passes is larger than drop evaporation time. Therefore when drops in one pass arrive at the bulk layer, separate crater holes have been already formed by the drops in the previous pass. The drops typically land on two crater holes thus the drop slip motion to a specific direction is weaker than that in the case of unidirectional printing with long time between adjacent drops (Fig.6(b)). Essentially multiple-pass printing improves the uniformity of multi-layer lines by attenuating the ink migration due to the slip motion of deposited drops.

Fabrication of Conductive Traces

Multi-layer lines printed with short or medium time between adjacent drops (Fig.4) result in open connection after the sintering process. Printing layer-by-layer with long time between adjacent drops either unidirectionally or bidirectionally makes the sintered lines electrically connected. However, it is severely detrimental to the manufacturing throughput due to the low printing efficiency (< 4 Hz). To overcome this dilemma in conductivity performance and manufacturing efficiency, an optimized multiple-pass printing routine is developed:

- Determine drop diameter D_0 after evaporation.
- Determine highest reliable jetting frequency f_{max}.
- Determine drop evaporation time t_e.
- Specify the dot spacing within a printed line d_s.
- Drop pitch in each pass d_p is selected to be the minimum multiple of the dot spacing d_s without having any drops printed at this drop pitch overlapped. A necessary condition is $d_p = nd_s > D_0 (n \in \mathbb{N}^*)$.
- The number of passes n_p is determined by d_p/d_s.
- Print at the highest jetting frequency f_{max} in each pass and ensure the time between any two consecutive passes is larger than the drop evaporation time t_e. While waiting for the drops in one pass to evaporate, one can print other patterns.

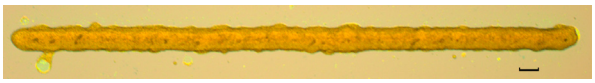

Figure 7. *A 15-layer line with dot spacing 40 μm using optimized 5-pass printing at a jetting frequency of 800 Hz. Experiments have shown that the highest reliable jetting frequency for the ink and the print head used in this study is about 800 Hz. The calibration bar represents 100 μm.*

The printed lines are sintered on a hot plate at 250°C for 1 h before further electrical characterization. The line resistances are measured using 2-probe method. Table 2 summarizes sheet resistance and required printing time for a 15-layer line with dot spacing 40 μm using different printing methods.

Table 2: Comparison of Different Printing Methods

Printing Methods	Sheet Resistance ($\Omega/\square$)	Print Time (s)
Unidirectional printing with 290 ms between adjacent drops	14.881 ± 0.741	326.3
Bidirectional printing with 290 ms between adjacent drops	14.268 ± 0.439	326.3
Optimized 5-pass printing @ 800 Hz	13.885 ± 0.411	1.3

The optimized 5-pass printing yields the lowest sheet resistance because the amount of ink migration by multiple-pass printing is minimal, which in turn results in the most uniform material distribution across a printed line. Moreover, in terms of printing efficiency, the optimized multiple-pass printing is two orders of magnitude better than the other two printing methods.

From the perspective of a general printing routine for fine conductive trace fabrication, there are several benefits to use optimized multiple-pass printing. First, printing is always operated at the highest reliable jetting frequency. Second, dot spacing and jetting frequency can be designed independently as opposed to the conventional one-pass printing where a correct combination of dot spacing and jetting frequency is required in order to achieve the line stability [5,7,8]. Third, minimum line width is ensured. Since the optimized multiple-pass printing ensures that every drop is deposited when its adjacent drops are dry, the line width is always about the drop diameter, which is the smallest length scale that can be produced by inkjet printing.

Conclusion

This paper presents an experiment-based study of printed line morphologies using volatile ink in the presence of contact angle hysteresis and non-zero receding contact angle. If a line is printed with short time between adjacent drops so that the contact line of the bead is still pinned as it merges with the arriving droplet, one or several agglomerations are formed in the middle of the line. If a line is printed with medium time between adjacent drops so that the bead is depinned from its contact line upon merging, only one agglomeration is formed and is always located at the end of the line. This is because the evaporation during the time between adjacent drops causes the molar concentration of the bead considerable higher than that of newly deposited drops, which results in a relatively lower surface tension of the bead because of positive surface excess of the solute. A flow induced by this surface tension gradient consistently drives the bead towards fresh deposited drops. If a line is printed with time between adjacent drops being longer than drop evaporation time, no agglomeration is observed. Multi-layer lines printed unidirectionally with short or medium time between adjacent drops have agglomerations, which is explained by the accumulation of agglomerations that take place at every layer. A multi-layer line printed unidirectionally with long time between adjacent drops exhibits nonuniformity with the beginning of the line appearing to be darker than its end. This is because deposited drops dissolve bulk layer, leaving a crater-like hole in the bulk and the drops consistently slip into the hole due to gravity. The uniformity of the line is improved by printing bidirectionally with long time between adjacent drops or using multiple-pass printing. Optimized multiple-pass printing is developed so that the printing is always operated at the highest reliable jetting frequency in each pass, yielding excellent print efficiency and electrical conductivity.

Acknowledgments

We thank Hewlett Packard for providing inkjet printing equipment. We thank Professor James D. Litster and Nathan B. Davis for surface tension measurement. We also thank J. William Boley for helpful discussions, Guoping Xiong and Stephen Hodson for microscope imaging assistance and ink preparation.

References

[1] C. Kim, M. Nogi, K. Suganuma, and Y. Yamato. Inkjet-Printed Lines with Well-Defined Morphologies and Low Electrical Resistance on Repellent Pore-Structured Polyimide Films. *ACS applied materials interfaces*, 2012.

[2] C. Kim, M. Nogi, and K. Suganuma. Electrical conductivity enhancement in inkjet-printed narrow lines through gradual heating. *Journal of Micromechanics and Microengineering*, 22(3):3–8, March 2012.

[3] H. Lee, K. Chou, and K. Huang. Inkjet printing of nanosized silver colloids. *Nanotechnology*, 16(10):2436–2441, October 2005.

[4] S. Davis. Moving contact lines and rivulet instabilities. Part 1. The static rivulet. *Journal of Fluid Mechanics*, 98(02):225–242, April 1980.

[5] P. Duineveld. The stability of ink-jet printed lines of liquid with zero receding contact angle on a homogeneous substrate. *Journal of Fluid Mechanics*, 477(-1):175–200, March 2003.

[6] J. Stringer and B. Derby. Limits to feature size and resolution in ink jet printing. *Journal of the European Ceramic Society*, 29(5):913–918, March 2009.

[7] J. Stringer and B. Derby. Formation and stability of lines produced by inkjet printing. *Langmuir The ACS Journal Of Surfaces And Colloids*, 26(12):10365–10372, June 2010.

[8] D. Soltman and V. Subramanian. Inkjet-printed line morphologies and temperature control of the coffee ring effect. *Langmuir The ACS Journal Of Surfaces And Colloids*, 24(5):2224–2231, 2008.

[9] P. Thomas and A. Lavanya. Self-assembling bilayers of palladiumthiolates in organic media. *Journal of Chemical Sciences*, 113(December):611–619, 2001.

[10] W. Boley, C. Shou, and G. Chiu. Drop coalescence for an inkjet printed functional film: how avoiding coalescence can improve functional performance (working paper).

[11] R. Deegan. Pattern formation in drying drops. *Physical Review E Statistical Physics Plasmas Fluids And Related Interdisciplinary Topics*, 61(1):475–85, 2000.

[12] A. Adamson. *Physical Chemistry of Surfaces 2nd Edition*. Interscience Publishers, New York, N.Y., 1967.

[13] N. Lange. *Lange's Handbook of Chemistry 10th Edition*. 1967.

[14] R. Deegan, O. Bakajin, T. Dupont, G. Huber, S. Nagel, and T. Witten. Capillary flow as the cause of ring stains from dried liquid drops. *Nature*, 389(6653):827–829, 1997.

[15] C. Shou. *A Study of Inkjet Printed Line Morphology Using Volatile Ink with Non-zero Receding Contact Angle for Conductive Trace Fabrication*. Master thesis, Purdue University, 2013.

[16] S. Schiaffino and A. Sonin. Formation and stability of liquid and molten beads on a solid surface. *Journal of Fluid Mechanics*, 343(-1):95–110, July 1997.

[17] S. David, K. Sefiane, and L. Tadrist. Experimental investigation of the effect of thermal properties of the substrate in the wetting and evaporation of sessile drops. *Colloids and Surfaces A Physicochemical and Engineering Aspects*, 298(1-2):108–114, April 2007.

[18] T. Kawase, H. Sirringhaus, R. Friend, and T. Shimoda. Inkjet Printed Via-Hole Interconnections and Resistors for All-Polymer Transistor Circuits. *Advanced Materials*, 13(21):1601–1605, November 2001.

[19] Y. Xia and R. Friend. Nonlithographic patterning through inkjet printing via holes. *Applied Physics Letters*, 90(25):253513, 2007.

[20] E. Tekin, B. Gans, and U. Schubert. Ink-jet printing of polymers-from single dots to thin film libraries. *Journal of Materials Chemistry*, 14(17):2627–2632, 2004.

Author Biography

Chenchao Shou received his BS in Engineering from Shanghai Jiao Tong University (2011) and his MS in Mechanical Engineering from Purdue University (2013). He is currently pursuing his PhD in Mechanical Science and Engineering at University of Illinois at Urbana-Champaign.